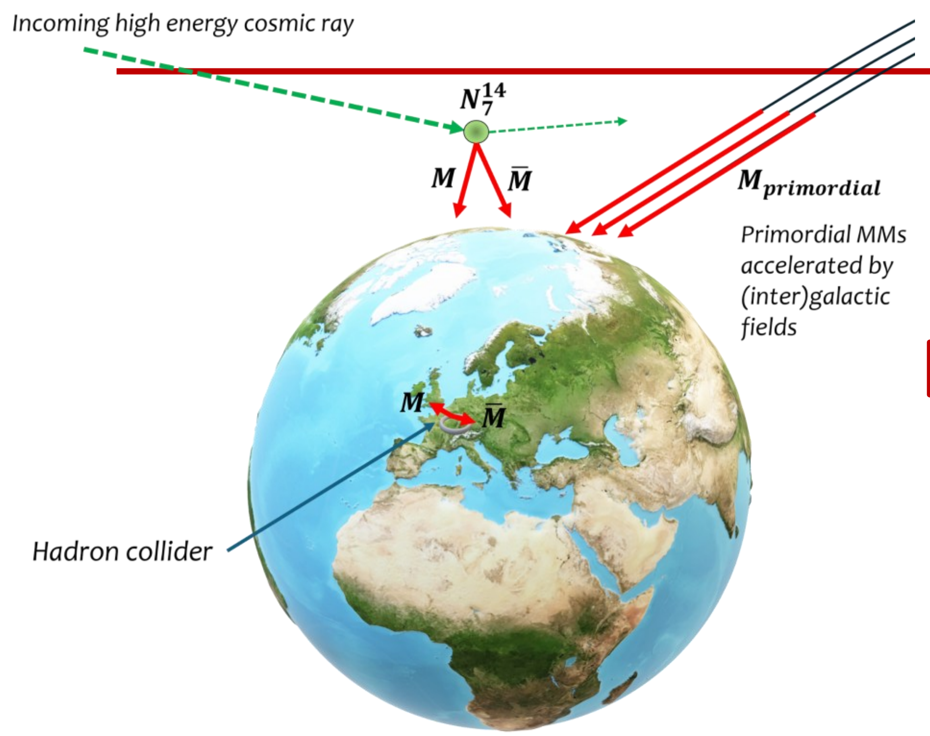

Nuclear track detectors for magnetic monopole searches in large area experiments

focus on some peculiar technical aspects of MACRO and SLIM

Maurizio Spurio
Università di Bologna and INFN
maurizio.spurio@unibo.it

ALMA MATER STUDIORUM UNIVERSITÀ DI BOLOGNA

INFN BOLOGNA

Nuclear Track Detectors (NTDs) [1]

- The passage of heavily ionizing particles may be permanently recorded in some insulating materials: plastic sheets as CR39, Lexan (Makrofol), glasses and to minerals like mica and obsidian (NTDs).
- NTDs are threshold devices, depending on the material and on chemical etching, with no time resolution.
- NTDs are sensitive to the fraction of the energy loss in a narrow region close to the particle's trajectory forming a ***latent track***

The breaking of polymeric chains of plastic NTD by a crossing particle [1]

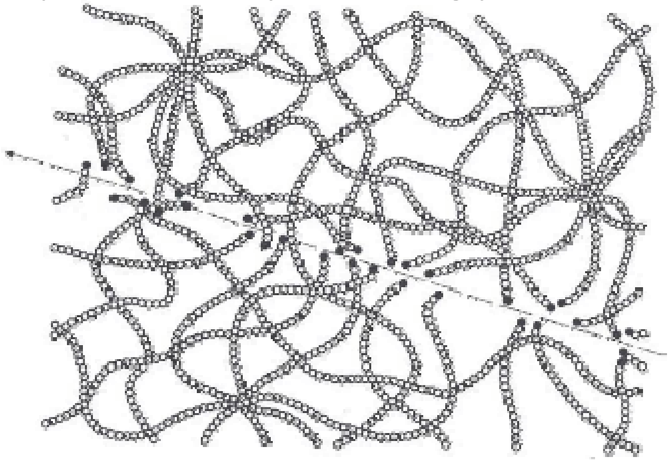

Nuclear Track Detectors (NTDs) [1]

- The passage of heavily ionizing particles may be permanently recorded in some insulating materials: plastic sheets as CR39, Lexan (Makrofol), glasses and to minerals like mica and obsidian (NTDs).
- NTDs are threshold devices, depending on the material and on chemical etching, with no time resolution.
- NTDs are sensitive to the fraction of the energy loss in a narrow region close to the particle's trajectory forming a ***latent track***

The breaking of polymeric chains of plastic NTD by a crossing particle [1]

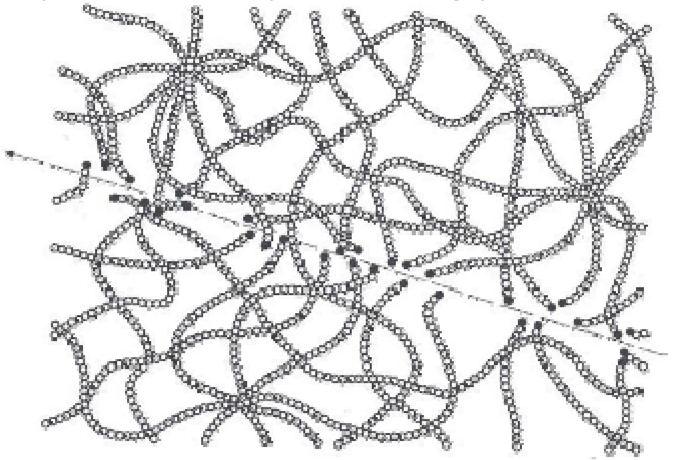

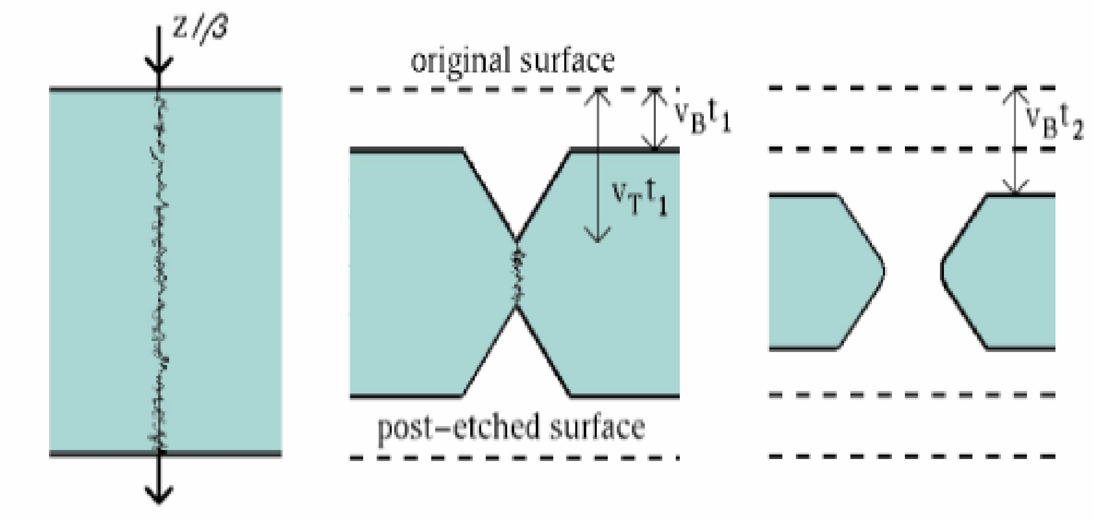

- The latent track may be made visible by proper chemical etching. The etching velocity along the latent track (v_T) is faster than the bulk etch rate (v_B).
- One may obtain a hole in a sheet of the sensitive material or two etched cones on each side of the sheet.
- The hole (or cone) in correspondence of the latent track may be detected by observation with optical microscopes

The restricted energy loss (REL)

- In NTDs (CR39, Lexan,…), the **restricted energy loss** (REL) is the relevant quantity for the latent track.
- The REL may be determined from the geometry of the etched cones. For CR39 this technique is particularly successful, yielding measurements of the electric charge of heavy relativistic nuclei ($Z > 5$) to a precision of 0.05e if several layers of plastic sheets are used.

The restricted energy loss (REL)

- In NTDs (CR39, Lexan,…), the **restricted energy loss** (REL) is the relevant quantity for the latent track.
- The REL may be determined from the geometry of the etched cones. For CR39 this technique is particularly successful, yielding measurements of the electric charge of heavy relativistic nuclei (Z > 5) to a precision of 0.05e if several layers of plastic sheets are used.

REL and Magnetic Monopoles

- The interaction between MMs ($\beta > 0.05$ and $\gamma \leq 100$) and the electrons of a material is well understood. The REL excludes the energy transfers in energetic δ-rays, i.e., in energy deposited far away from the latent track.
- For MM with $\beta < 10^{-2}$, elastic collisions with the target atoms and molecules, where the lost energy goes to the recoiling target nucleus, must be considered.
- The detailed computation relies on computer codes

REL in CR39 vs. β for MMs with 1,2 and 3 g_D [3]

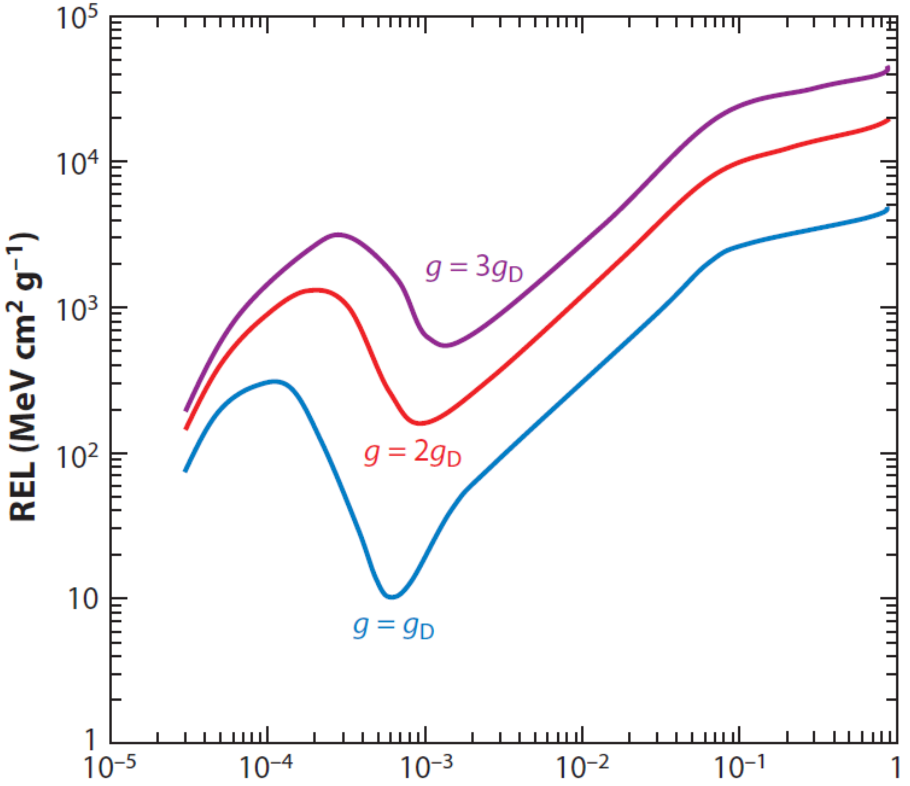

$$\beta = \frac{v}{c}$$

p → REL → dE/dx [2,13]

1. From the energy loss, the REL can be computed
2. The geometrical parameters of the track depend on the REL.
3. From the measurement of the track parameters, we can construct a calibration curve p vs. REL

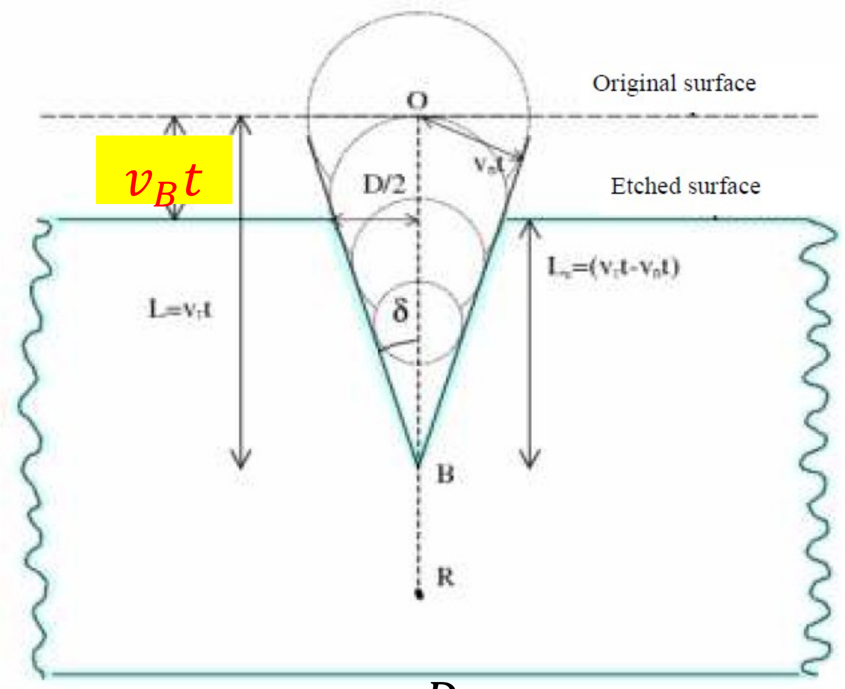

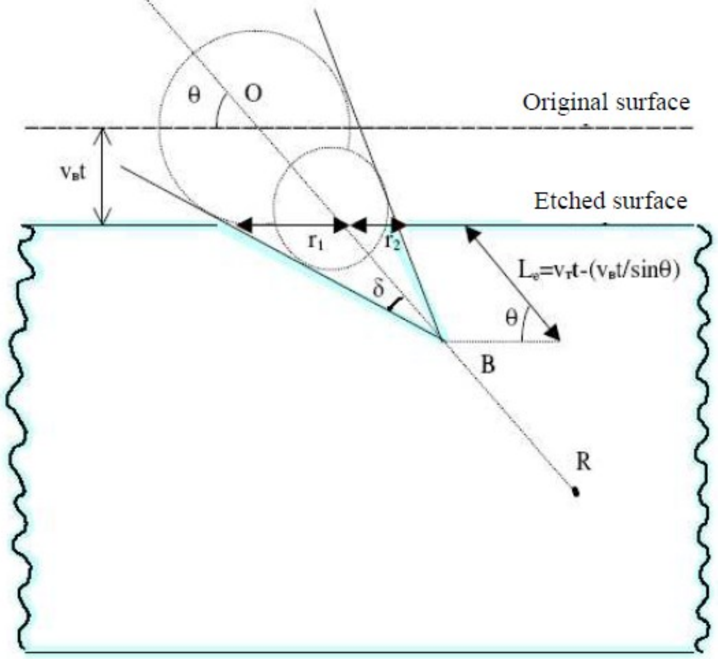

$$p \equiv \frac{1+(\frac{D}{2v_B t})^2}{1-(\frac{D}{2v_B t})^2}$$

$$p \equiv f(D,d)\,; \quad \vartheta = g(\mathrm{p},\mathrm{d})$$

The INTERCAST CR39 (MACRO and SLIM)

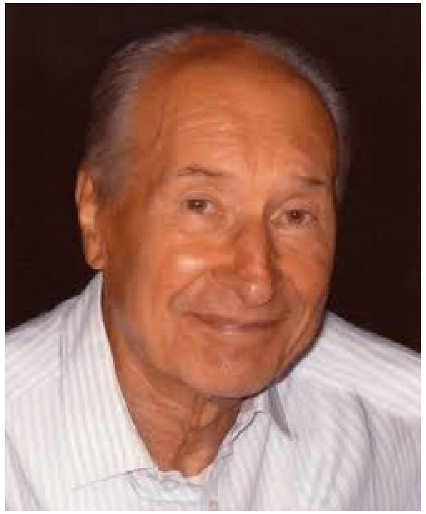

- The Bologna group, lead by prof. **G. Giacomelli**, started the research using NTD in 1986, having the responsibility of the NTD used in MACRO and SLIM experiments.
- The was possible because a research-based collaboration with a close by Industry (Intercast Europe Co. of Parma) who manufactured our CR39 **from 1986 until 1999**.
- A **specific production line was set up** to achieve the controlled conditions to reach low detection threshold, high sensitivity in a large range of energy losses, high quality of the post-etched surface after prolonged etching and stability of the detector response over long periods of time.
- Two types of CR39 have been developed, containing different additives and using **different catalyzers** and **curing cycles**: the EN3 type (used in the 1st MACRO supermodule) and the L6 type, that was installed in all the rest of MACRO and used in the SLIM experiment.
- The **EN3** type CR39 (*optimized for neutron dosimetry*) was produced using the CHPC catalyzer, the DOP additive and a curing cycle with a maximum temperature of 80°C.
- The **L6** version (*optimized for MM detection*) is produced using the IPP catalyzer, the Naugard N445 antioxidant additive and a curing cycle with a maximum temperature of 95°C.
- INTERCAST was acquired by PPG Industries in 2006, relocated to Thailand and closed in 2012.

Calibration of the CR39 [5,8,11]

- To establish the response NTD, stacks of CR39 sheets were exposed to **relativistic ions**:
  - 16 A GeV O16+ @ Brookhaven (1988)
  - 0.585 A GeV Ne10+ @ Berkeley (1990)
  - 14.5 A GeV Si14+ @ Brookhaven (1990)
  - 200 A GeV S16+ @ CERN (1990)
  - 11.3 A GeV Au79+ @ Brookhaven (1992)
  - 158 A GeV Pb82^{+} and In49^{+} @CERN-SPS (1994,1996)
  - 1 A and 5A GeV Fe26^{+} @ BNL-AGS (1999, 2005)
  - ….
- CR39 sheets (7 x 13) cm^2 in size of CR39, thickness 1.4 mm, located before and after a Cu / Al /… target were exposed to a total flux of ~1500 ions/cm^2
- Both the primary ions and their fragments have been used for the calibrations.

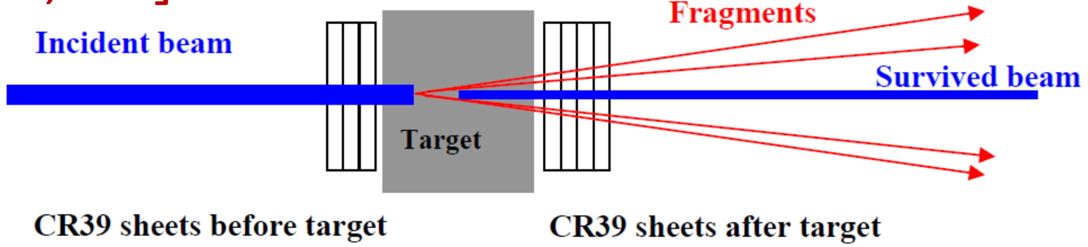

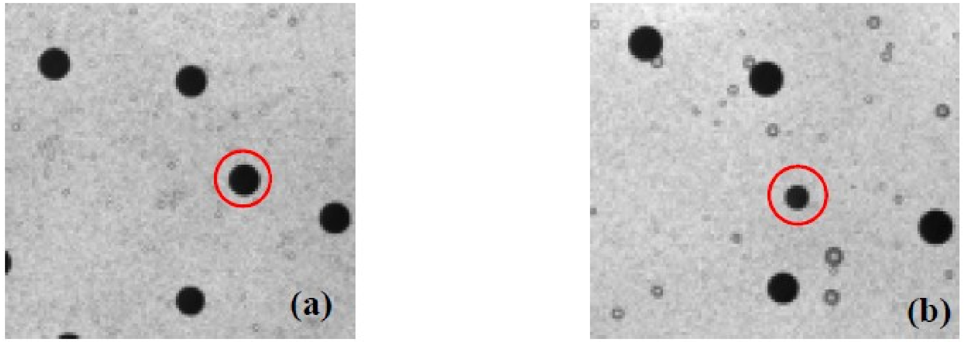

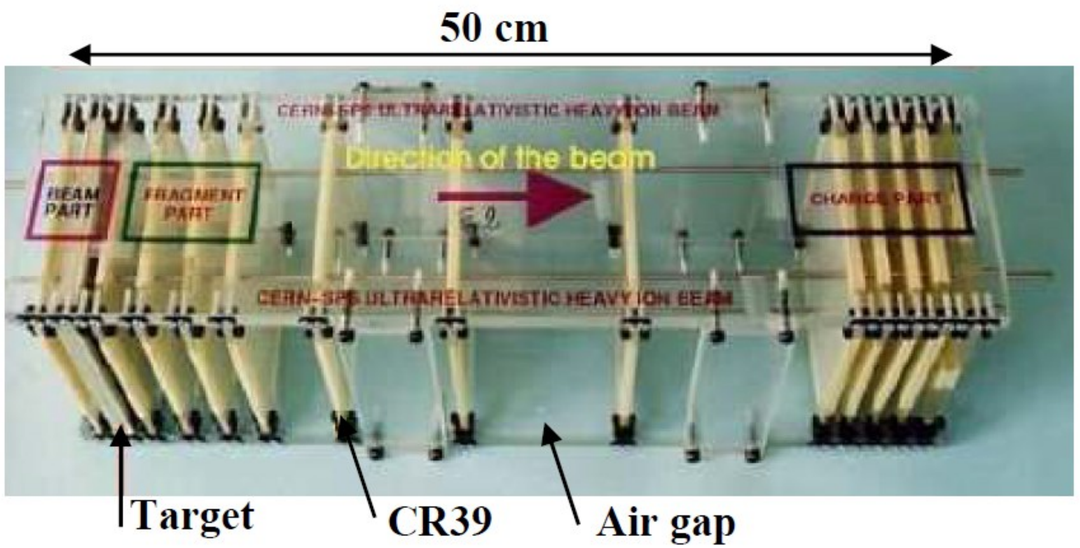

Calibration of the CR39 with relativistic ions

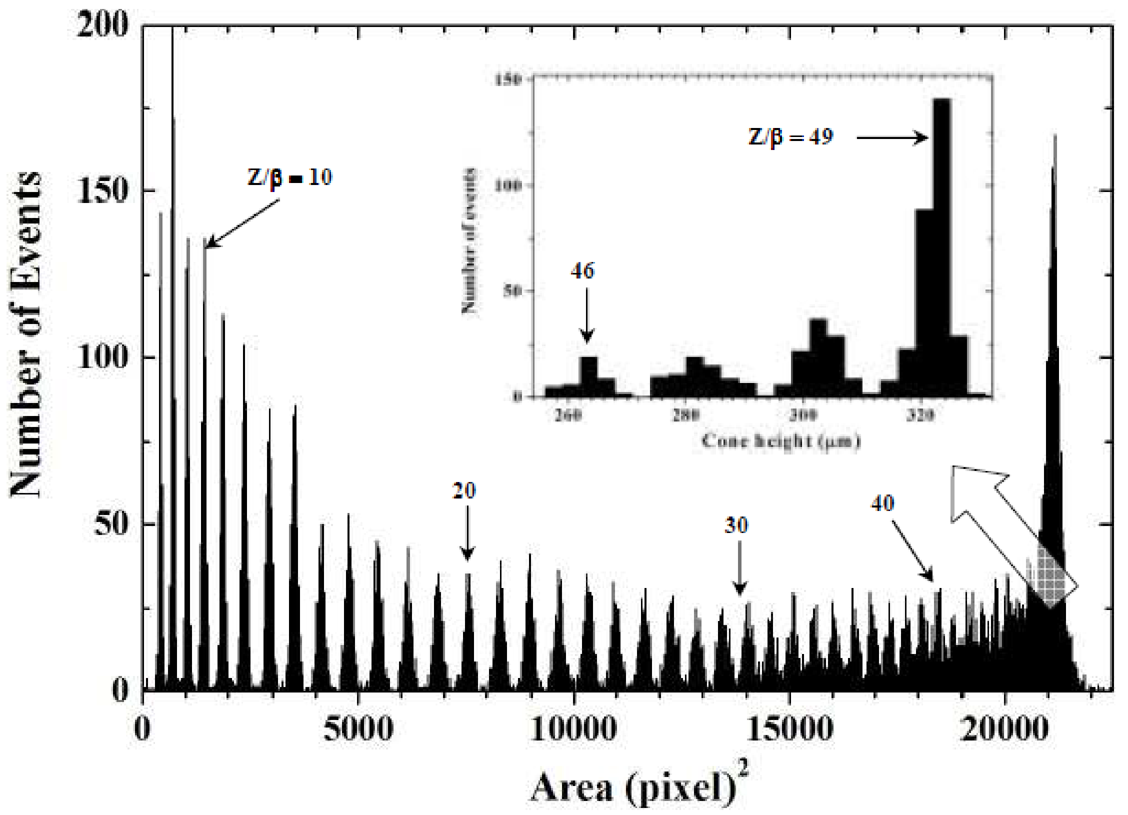

Base area distribution of etched cones in CR30 from In49 ions and their fragments (averages of 2 front face measurements); Inset: cone height distribution for 46≤ Z ≤ 49 (single measurements) using the soft etching

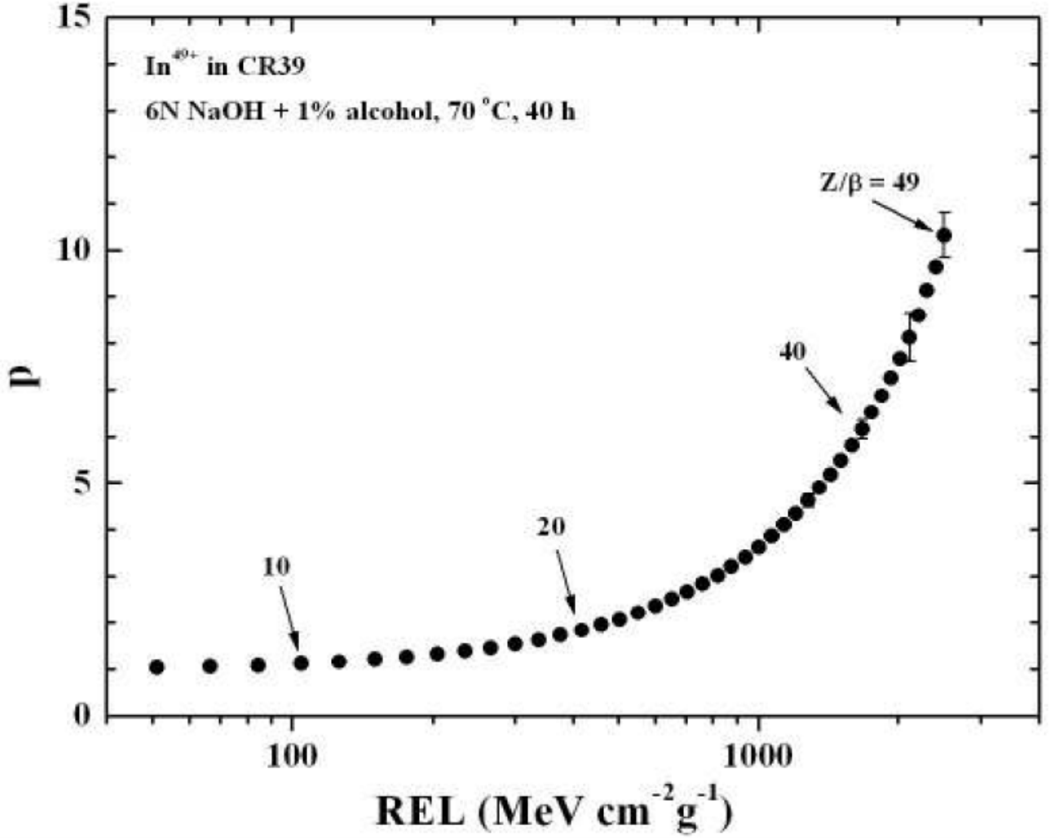

The etch rate ratio p plotted as a function of REL for CR39 detectors exposed to In^{49} using the measered p. Typical statistical standard deviations are shown at Z/β = 40, 45, 49; for Z/β ≤ 37 the errors are inside the black points.

Calibration of the CR39- low energies [5]

- At low-energy ($\beta \sim 10^{-4}$-10^{-2}), nuclear stopping S_n becomes important w.r.t. electronic stopping S_e
- In 1992, Snowden-Ifft and Price [PLB 288, 250] found that for a particular type of CR-39 the S_n appeared to be only 20% as effective as S_e in track formation.
- The S_n and S_e can be calculated using computer codes. In the fig. , results from the 1990 version of the TRIM code on semi-empirical theory of energy loss of ions in solids [6].
- The S_n for p and D (100 A keV), and Be (300KeV) ions are a small fraction of the total; that for Si (200-400 keV) is 50%-30%. These were used to determine the contribution to the response of the nuclear energy loss.

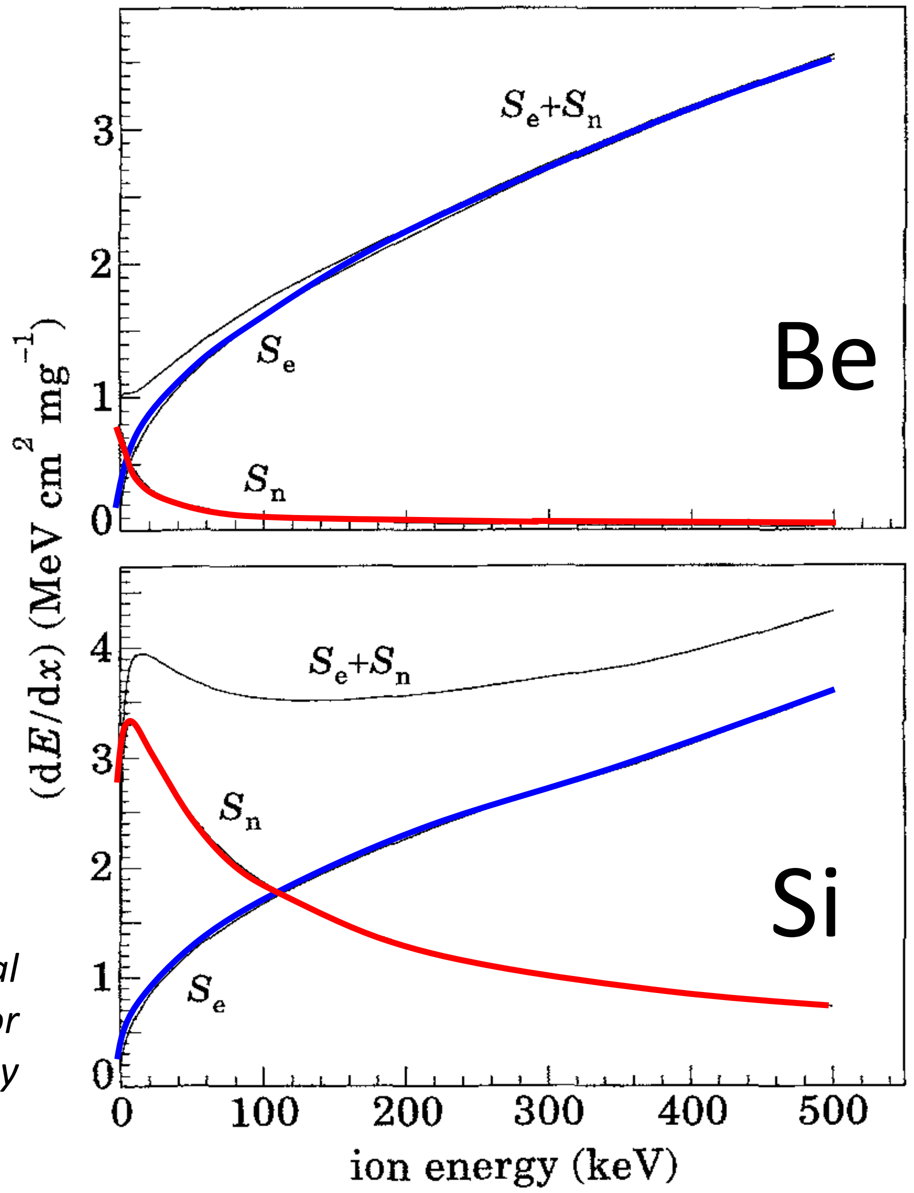

The predictions of the TRIM program for the differential electronic (S_e), nuclear (S_n) and total (S_e + S_n) energy losses for beryllium and silicon ions in CR39 vs. ion kinetic energy

Calibration of the CR39- low energies [5]

- To measure tracks produced by low-energy ions, plastic replicas of the etch pits were produded and observed with a Scanning Electron Microscope (SEM).
- **The results we obtained are compatible with a 100% contribution of S_n to the CR39 response**.
- The result (relevant for the search for MM with galactic velocities) was confirmed with a different CR39 and analysis method by an American group [7]

IL NUOVO CIMENTO VOL. 109 A, N. 8 Agosto 1996

Calibration with relativistic and low-velocity ions of a CR39 nuclear track detector

Measured reduced etch rate p vs REL for the CR39 exposed to relativistic and slow ion beams; the points are the experimental data, the solid line is the best fit to the data points (8 < Z < 68) obtained with relativistic ions

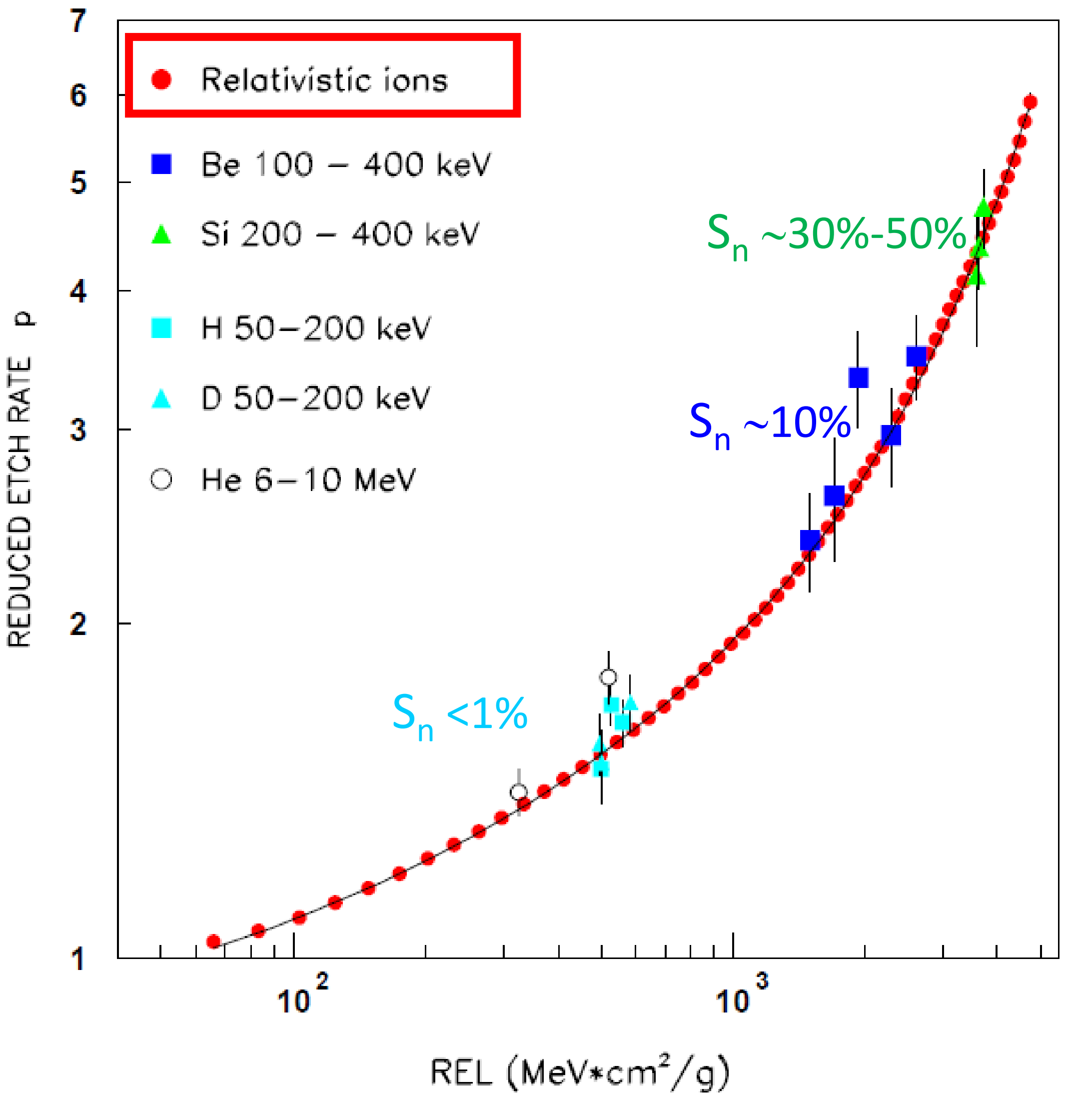

The MACRO@LNGS (1989-2000)

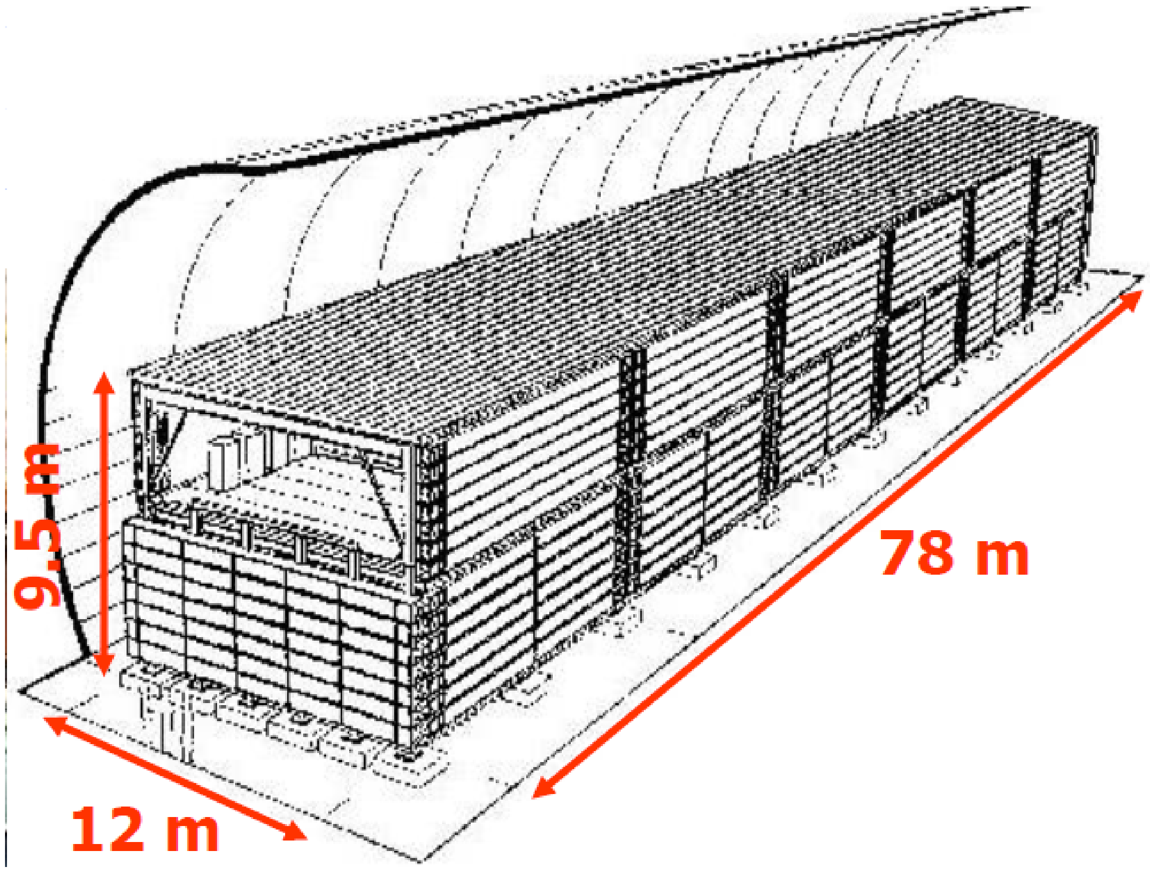

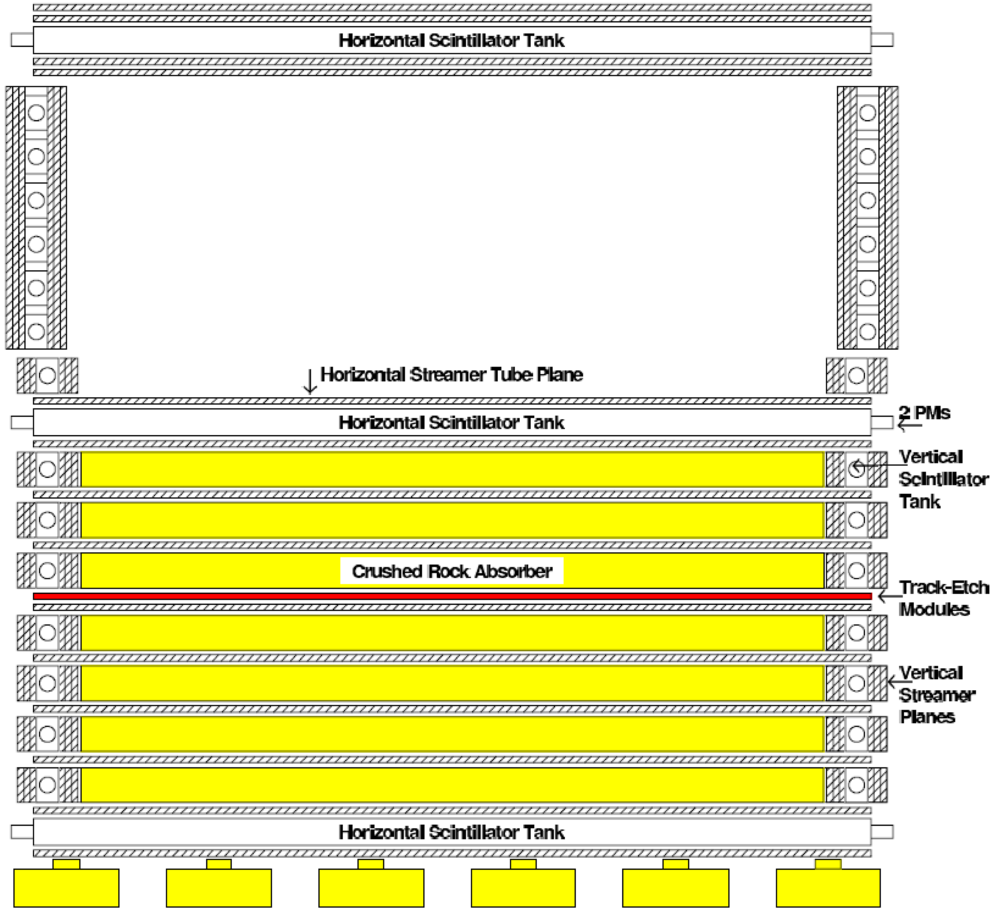

- Very wide β range of MM velocities
- Redundancy & Complementarity (for a single event detection) **[4]**

The MACRO@LNGS and the NTD

- The MACRO NTD was distributed in three orthogonal planes for a total area of **1263** m^2
- It is assembled in **24.5×24.5 cm^2** “wagons”: **13,536** in the horizontal; **7824** in two vertical planes.
- Each “wagon” contains 3 CR39 layers, each 1.4 mm thick (labelled L1, L3, L5), 3 layers of Lexan (0.25 mm thick and an Aluminium absorber, 1 mm thick.
- Each stack is placed in an aluminized mylar bag filled with dry air.

The MACRO@LNGS and the NTD

- The MACRO NTD was distributed in three orthogonal planes for a total area of **1263** m^2
- It is assembled in **24.5×24.5 cm²** “wagons”: **13,536** in the horizontal; **7824** in two vertical planes.
- Each “wagon” contains 3 CR39 layers, each 1.4 mm thick (labelled L1, L3, L5), 3 layers of Lexan (0.25 mm thick and an Aluminium absorber, 1 mm thick.
- Each stack is placed in an aluminized mylar bag filled with dry air.

- After extraction from the apparatus, three fiducial holes of 2 mm diameter were drilled in each “wagon” (100 μm accuracy). The aluminized mylar bags are open and the detectors are labelled.
- Chemical etching is done in a steel thermostatic tank where **24 foils** (6 linear m=one “train” in the following) are assembled inside a steel basket: 1.44 m^2 of detectors are etched together.

MACRO: searching for Monopoles-I

- A “strong” etching in a 8 N NaOH water solution at 80–90◦C is performed: thickness of each foil is about 300–400 μm (50–90 h of etching time) with a v_B ~5–10 μm/h.
- **Signal**: a hole or a biconical track with the two base-cone areas equal within experimental uncertainties.
- **Calibration**: using Fe ions at 0°, 30°, 45° the minor axes on the front (F) and back side (B) of each sheet were measured, obtaining a ratio **F/B=1.00 ± 0.02** (3 standard deviations) for all angles.
- **Search**: the L1 sheets were scanned twice by different operators with a 3× magnification optical lens (the time for each scan is about 15 h/“train”) looking for any possible optical inhomogeneity.

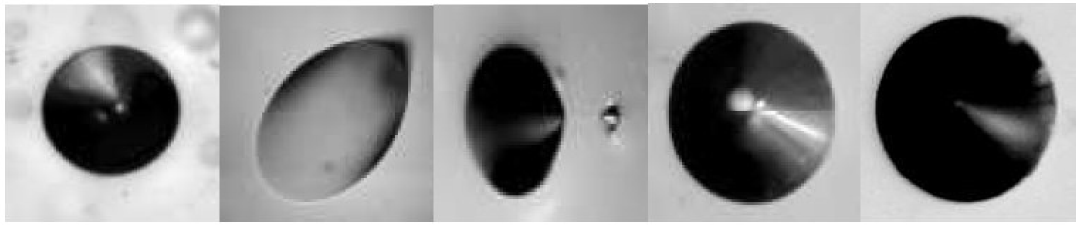

Figure: Different track shapes as observed in the L1 sheet after strong etching

MACRO: searching for Monopoles-I

- A "strong" etching in a 8 N NaOH water solution at 80–90◦C is performed: thickness of each foil is about 300–400 μm (50–90 h of etching time) with a v_B ~5–10 μm/h.
- **Signal**: a hole or a biconical track with the two base-cone areas equal within experimental uncertainties.
- **Calibration**: using Fe ions at 0°, 30°, 45° the minor axes on the front (F) and back side (B) of each sheet were measured, obtaining a ratio **F/B=1.00 ± 0.02** (3 standard deviations) for all angles.
- **Search**: the L1 sheets were scanned twice by different operators with a 3× magnification optical lens (the time for each scan is about 15 h/"train") looking for any possible optical inhomogeneity.

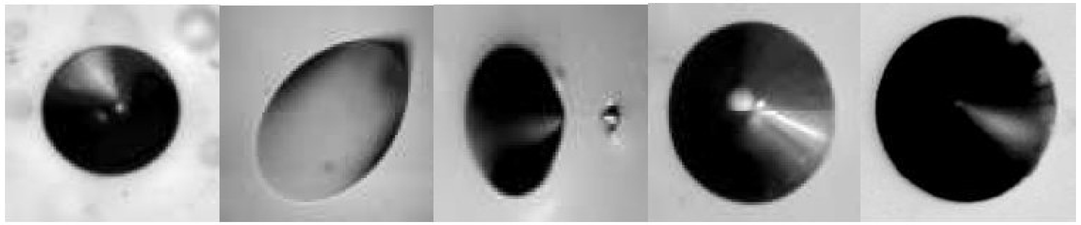

Figure: Different track shapes as observed in the L1 sheet after strong etching

- About 10–20 inhomogeneities were found per "wagon". An optical inhomogeneity is usually a particle track or a defect of the material. The double scan guarantees an efficiency of ~ 100% for a signal.
- Each detected inhomogeneity was observed with a stereo 40× microscope. About 10% of them were classified as track candidate and require further analyses. This second phase takes about 2.0 h/"train".

MACRO: searching for Monopoles-II

- Each track candidate (1–2 / "wagon") is observed under an optical microscope with larger magnification and the minor axis of the base-cone ellipse, in the front (a_F) and the back (a_B) sides is measured.
- For the selection of a "passing track" it is required that $\left|\frac{a_F}{a_B} - 1\right| \leq 3\sigma$.
- About 20% of the tracks passed, i.e. few per "train" of 6 m of CR39.

MACRO: searching for Monopoles-II

- Each track candidate (1–2 / “wagon”) is observed under an optical microscope with larger magnification and the minor axis of the base-cone ellipse, in the front (a_F) and the back (a_B) sides is measured.
- For the selection of a “passing track” it is required that $\left|\frac{a_F}{a_B} - 1\right| \leq 3\sigma$.
- About 20% of the tracks passed, i.e. few per “train” of 6 m of CR39.
- Then, the track major axes were measured to compute the $\boldsymbol{p} = \frac{\boldsymbol{v_T}}{\boldsymbol{v_B}}$ and **incident angles θ** for the front and back sides.
- A MM “**L1 candidate**” was defined if p and θ on the front and back sides are equal within 15%.

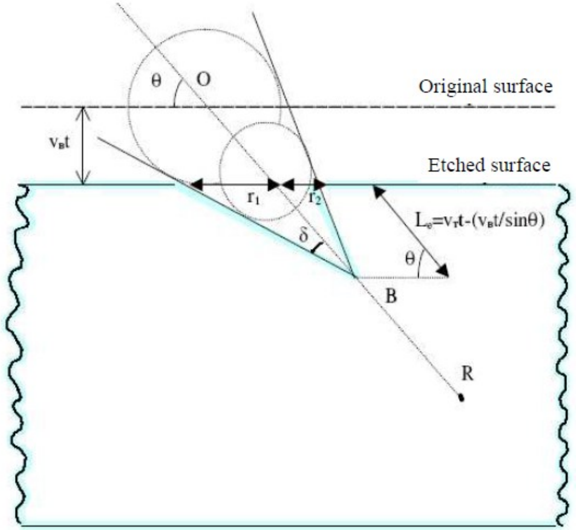

MACRO: searching for Monopoles-II

- Each track candidate (1–2 / "wagon") is observed under an optical microscope with larger magnification and the minor axis of the base-cone ellipse, in the front (a_F) and the back (a_B) sides is measured.
- For the selection of a "passing track" it is required that $\left|\frac{a_F}{a_B} - 1\right| \leq 3\sigma$.
- About 20% of the tracks passed, i.e. few per "train" of 6 m of CR39.
- Then, the track major axes were measured to compute the $\boldsymbol{p} = \frac{\boldsymbol{v_T}}{\boldsymbol{v_B}}$ and **incident angles θ** for the front and back sides.
- A MM "**L1 candidate**" was defined if p and θ on the front and back sides are equal within 15%.

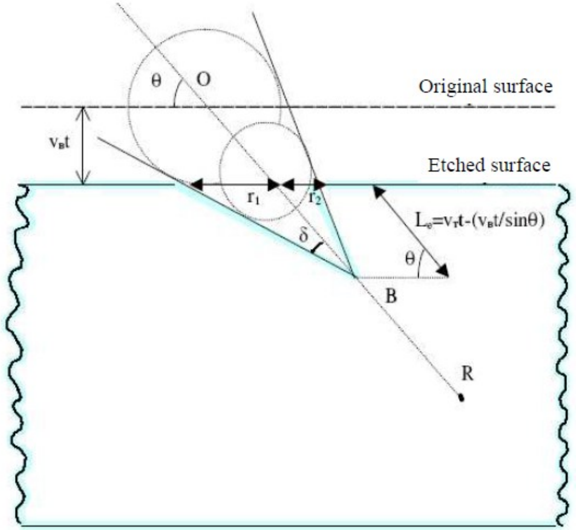

- To be a real **MM candidate**, a coincidence in **positions**, **angles** and **RELs** (i.e., ***p***) is required in the corresponding CR-39 L5 sheet and, if a coincidence is found, also in the L3 layer.
- The CR-39 L5 sheet is etched as the calibration stacks ("normal" etching: 6 N NaOH at 70◦C)
- The number of L5 sheets analyzed is 5–10% of the L1 sample.
- Using the incident direction of "L1 candidate" with its uncertainty, an area of about 1–2 cm^2 is selected in the L5 layer. This area is accurately scanned under an optical microscope with high magnification.

MACRO: searching for Monopoles-III [4]

- With “normal” etching, the track p-value (and the REL) could be estimated with an accuracy of 10%.
- No two-fold coincidence has been found, that is **no MM** (nuclearite or Q-ball candidate) **was observed**.

- The 90% CL upper limit was computed as

$$\Phi = \frac{2.3}{S\Omega\, T}$$

- $S\Omega$ is the acceptance of the “wagons” to MM and T is the “wagon” exposure time.
- Since the limits corresponding to each individual extraction are independent, the resulting MACRO CR-39 limit is given by the sum of each individual $S\Omega\, T$ contributions.
- For β~1, the solid angle Ω ~2.5-3.0 sr

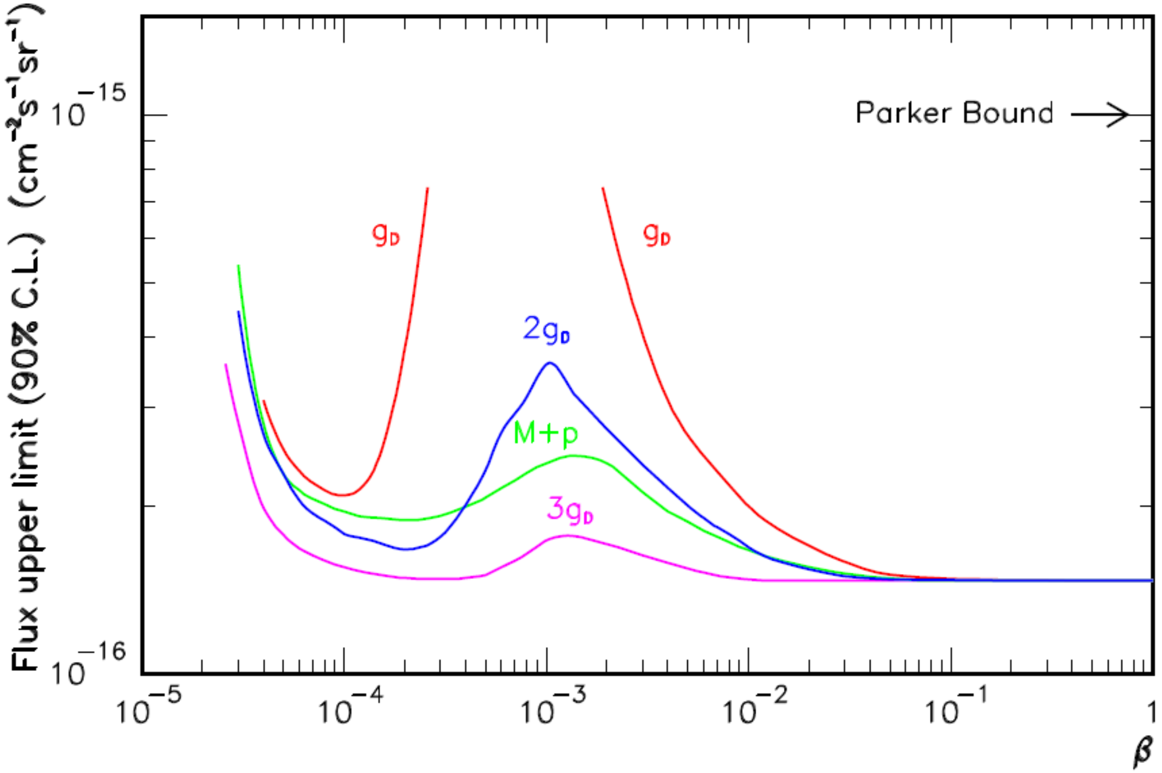

(a) Upper limits (90% CL) for an isotropic flux of MMs from the CR39 subdetector of MACRO for MM with g=1,2,3g_D and for M+p composites. https://arxiv.org/abs/0812.1105

The transition MACRO-SLIM

- Intermediate mass monopoles (IMMs), masses around 10^6–10^{10} GeV predicted by a phase transition in the early universe in which a gauge group yields a U(1) factor at a lower energy scale, required a different search.
- The SLIM experiment at a high-altitude laboratory (4300 m a.s.l.) allows to search for downgoing IMMs

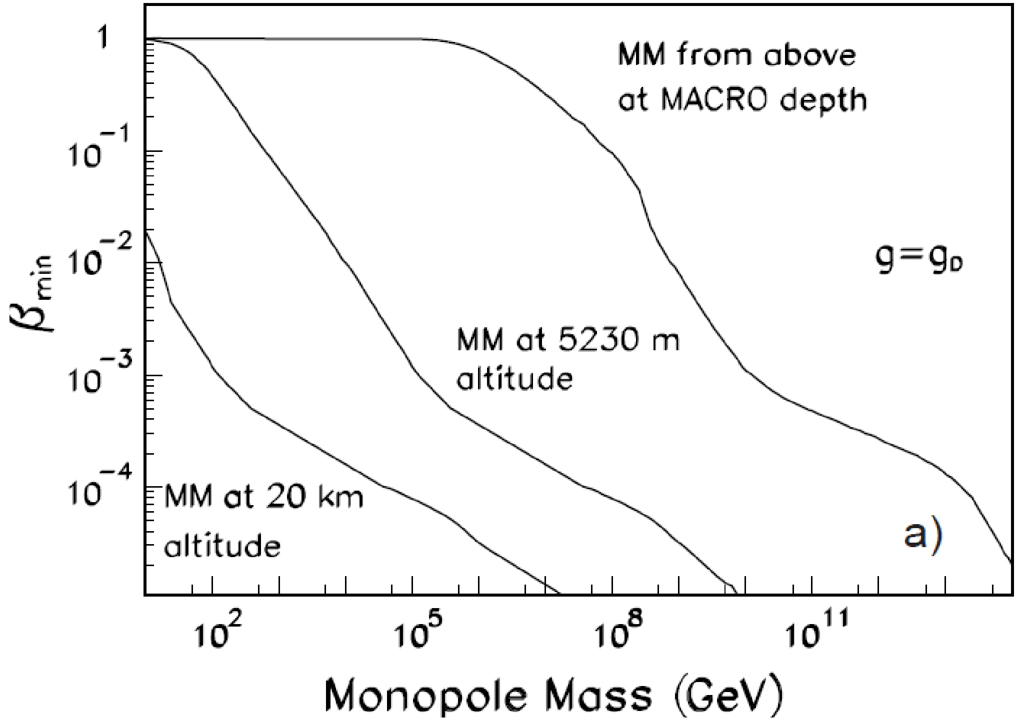

Accessible regions in the plane (mass, β) for monopoles with magnetic charge $g = g_D$ coming from above for an experiment at altitudes of 20 km, 5230 m, and for MACRO.

The SLIM experiment [9]

- The SLIM experiment was a 400m^2 array of NTDs2
- The array was organized into 7410 modules, each 24×24 cm^2.
- Installation started in February 2000 and ended in February 2002. The return of the material to Bologna was organized in batches, after the completion of the 4 years exposure.

The SLIM experiment [9]

- The SLIM experiment was a 400m^2 array of NTDs2
- The array was organized into 7410 modules, each 24×24 cm^2.
- Installation started in February 2000 and ended in February 2002. The return of the material to Bologna was organized in batches, after the completion of the 4 years exposure.

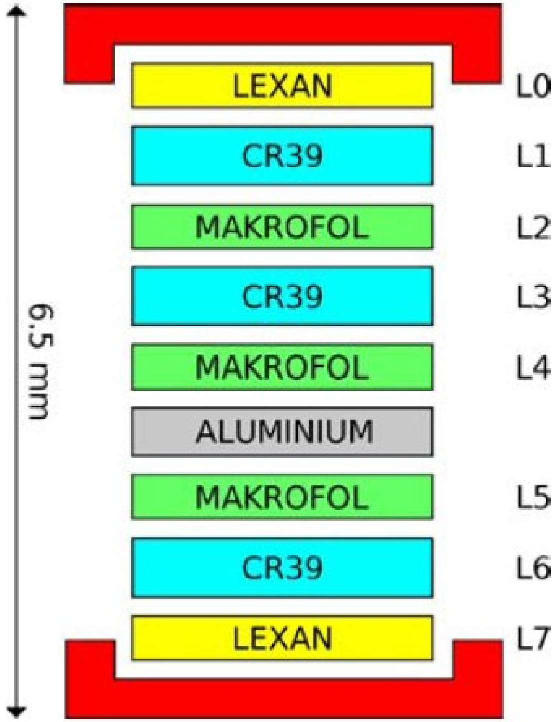

- All modules were made up of: three layers (1.4 mm thick) of CR39; 3 layers (0.48 mm) of Makrofol; 2 layers (0.25 mm) of Lexan each 0.25mm thick and one layer (1 mm) of aluminum absorber.
- Used the same CR39 as MACRO. But **environment different….**
- Neutron background: measured in the energy range of a few hundred keV to about 20 MeV: $\Phi_n = (1.7 \pm 0.8) 10^{-2}\ \mathrm{cm}^{-2}\mathrm{s}^{-1}$
- To reduce the neutron induced background in CR39 required to study **special etching procedures**, mainly based on the addition of ethyl alcohol to the etching solutions.

SLIM CR39 etching conditions [9]

- After >4y exposure at Chacaltaya the modules were brought back to be etched and analyzed in Bologna
- Etching the uppermost CR39 sheet using strong conditions

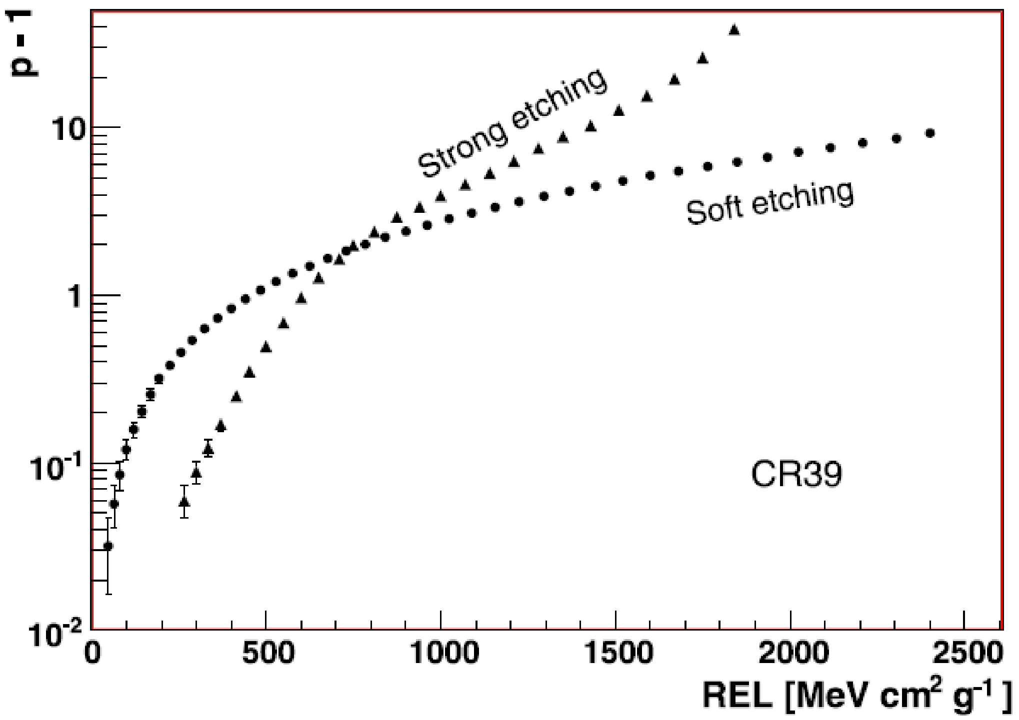

- "**Strong etching**" allows better surface quality and larger post-etched cones to be obtained.
- Used to analyze the top-most CR39 sheet in each module: etch pits easier to detect under visual scanning.
  - 8N KOH+1.5% ethyl alcohol at 75 ◦C for 30 h.
  - The bulk etching velocities was v_B = 7.2±0.4 μm/h (about 0.4-0.5 mm of CR39 removed)
- "**Soft etching**" applied to the other CR39 layers in a module if a candidate track was found after the first scan.
  - 6N NaOH+1% ethyl alcohol at 70 ◦C for 40 h
  - The bulk etching rates was v_B = 1.25±0.02 μm/h (about 0.1 mm of CR39 removed)

Searching for MM candidates [9]

- After etching CR39 sheet was scanned twice, with a stereo microscope, by different operators, with a 3×
- Further observation of a "suspicious correspondence" was made with an optical 20–40× stereo microscope and classified either as a **defect** or a **candidate track**.
- "**Candidate**": if the computed p and incident angle θ on the front/back sides equal to 20%. Then, the azimuth angle ϕ and its position P were also determined. The uncertainties Δθ, Δϕ and ΔP defined a "coincidence" area (< 0.5 cm^2) around the candidate expected position in the other layers

Searching for MM candidates [9]

- After etching CR39 sheet was scanned twice, with a stereo microscope, by different operators, with a 3×
- Further observation of a “suspicious correspondence” was made with an optical 20–40× stereo microscope and classified either as a **defect** or a **candidate track**.
- “**Candidate**”: if the computed p and incident angle θ on the front/back sides equal to 20%. Then, the azimuth angle ϕ and its position P were also determined. The uncertainties Δθ, Δϕ and ΔP defined a “coincidence” area (< 0.5 cm^2) around the candidate expected position in the other layers
- The lowermost CR39 layer soft etched; scan under an optical microscope with high magnification (500× or 1000×) in the region around the candidate expected position, which included the “coincidence” area.
- If a two-fold coincidence was detected, the CR39middle layer was also analyzed.
- The bottom CR39 sheet was etched in about 50 cases; the third CR39 sheet was etched only in few cases
- No events (although a fake candidate) and upper limits set

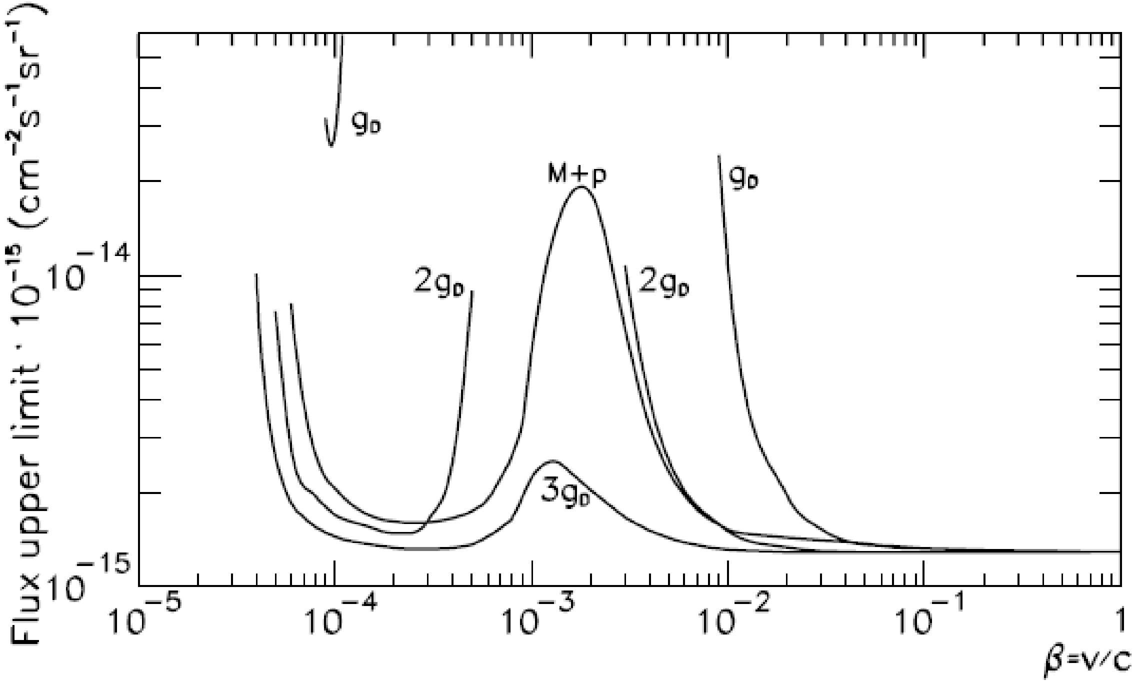

A fake candidate [10]

- In 2006 we observed an unexpected signal on the upper face of L1 CR39 layer (stack 7408): a sequence of etch-pits ("event") on the surface along a 20 cm line; each of them looked complicated (and possibly with many prongs)
- All the CR39 and Makrofol sheets in stack 7408 were analyzed, as well as 48 stacks surrounding it.
- A second sequence of etch-pits in the bottom layer (top face) of module 7410. These two abnormal events were of a kind never seen before.
- A study of the evolution of the etch-pits with increased etching time of the second candidate lends support to the interpretation that were fakes arising from detector defects
- The defects originated during the manufacture of the CR39 polymer. The monomer solution is poured within two casting glass plates separated by a gasket. At the end of the curing cycle, when the casting moulds are open, needle-like pieces of not perfectly cured material of microscopic size around the gasket have been accidentally deposited on the glass moulds and become a superficial inclusion in the polymer.

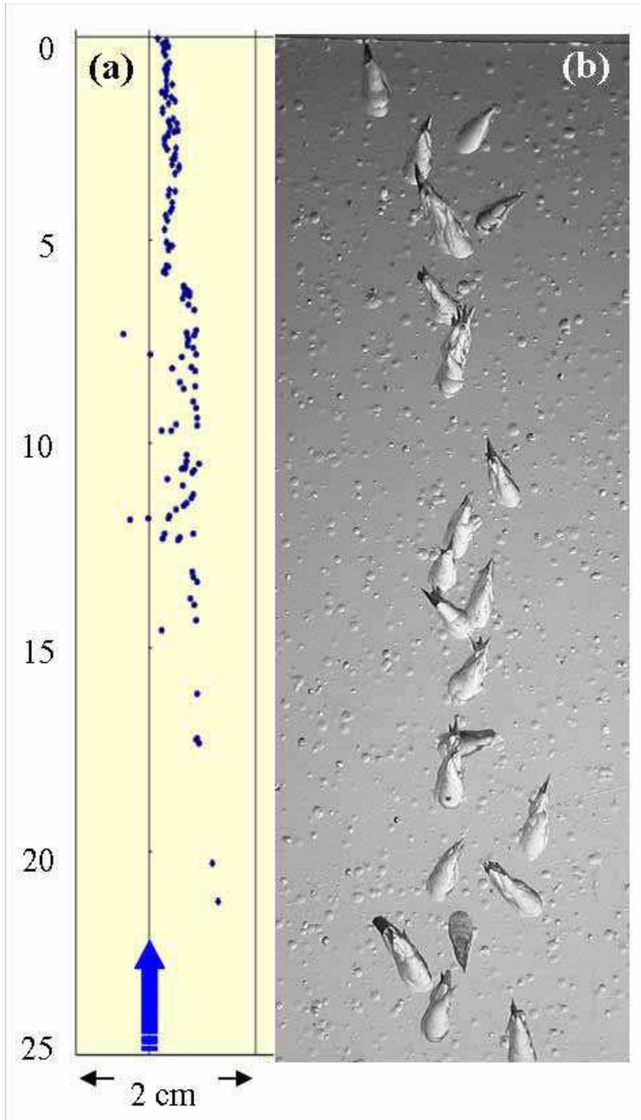

The aging effects of CR39 [8]

- The MACRO and SLIM CR39 was produced (1986-1999) in different batches (slight differences).
- The long exposure times for MM searches require the knowledge of aging and fading effects.
- The **aging is the loss of capability of detection in the period between the production and the exposure**.
  - To evaluate the aging, we studied the response of CR39 exposed to ion beams at different times after production and analyzed immediately after exposure.

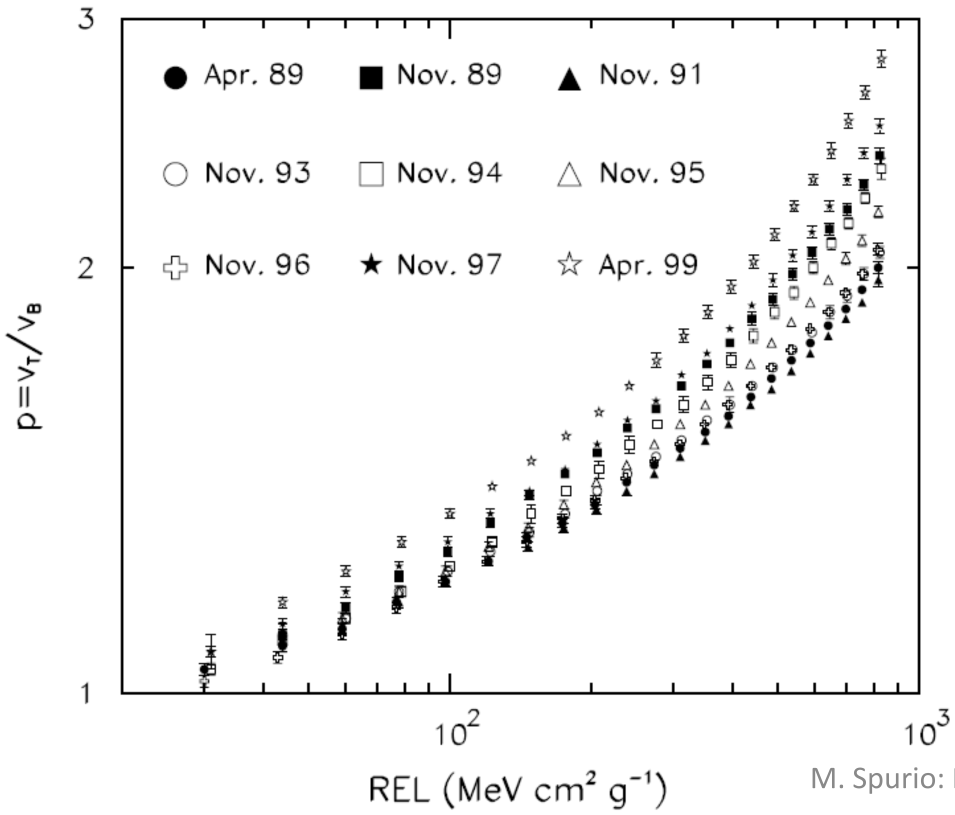

- Calibration curves (p vs REL) for various CR-39 production batches using the BNL-AGS Fe26+ beam of 1 A GeV in 1999.
- Each production batch has its own calibration curve with no evident connection with the production time (e.g., the calibration curves of **Nov. 89** and Nov. 97 production batches that are very similar.)
- The variation is mainly due to not perfectly identical conditions during the production

The aging effects of CR39 [8]

- The MACRO and SLIM CR39 was produced (1986-1999) in different batches (slight differences).
- The long exposure times for MM searches require the knowledge of aging and fading effects.
- The **aging is the loss of capability of detection in the period between the production and the exposure**.
  - To evaluate the aging, we studied the response of CR39 exposed to ion beams at different times after production and analyzed immediately after exposure.

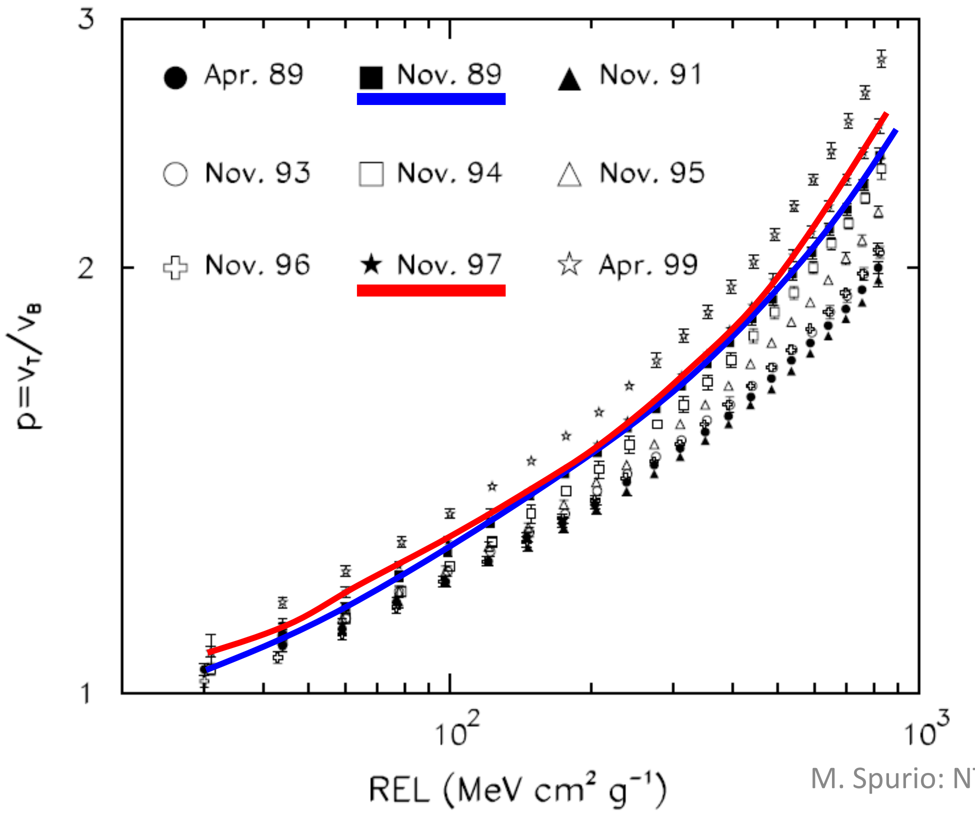

- Calibration curves (p vs REL) for various CR-39 production batches using the BNL-AGS Fe26+ beam of 1 A GeV in 1999.
- Each production batch has its own calibration curve with no evident connection with the production time (e.g., the calibration curves of **Nov. 89** and Nov. 97 production batches that are very similar.)
- The variation is mainly due to not perfectly identical conditions during the production

The aging effects of CR39 [8]

- The MACRO and SLIM CR39 was produced (1986-1999) in different batches (slight differences).
- The long exposure times for MM searches require the knowledge of aging and fading effects.
- The **aging is the loss of capability of detection in the period between the production and the exposure**.
  - To evaluate the aging, we studied the response of CR39 exposed to ion beams at different times after production and analyzed immediately after exposure.

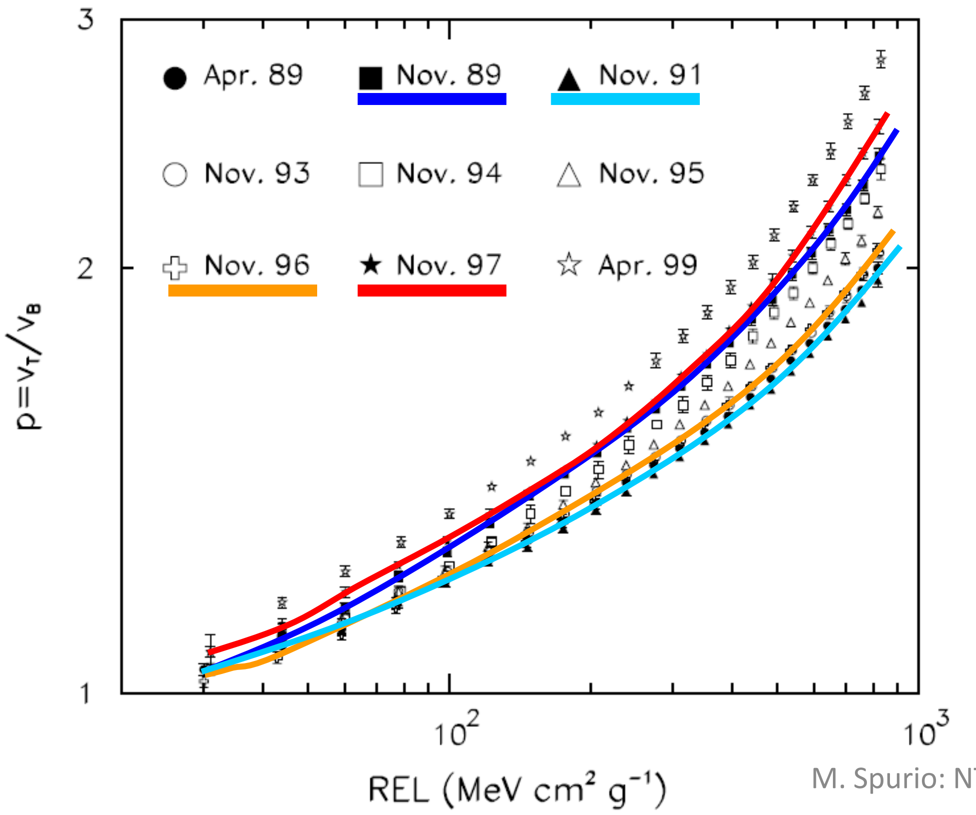

- Calibration curves (p vs REL) for various CR-39 production batches using the BNL-AGS Fe26+ beam of 1 A GeV in 1999.
- Each production batch has its own calibration curve with no evident connection with the production time (e.g., the calibration curves of **Nov. 89** and Nov. 97 production batches that are very similar.)
- The variation is mainly due to not perfectly identical conditions during the production

The fading effects of CR39 [8]

- The **fading** **is the partial or total loss of the damage due to a highly ionizing particle in the time elapsed from exposure to analysis**.
  - For the fading effect we compared the CR-39 response in sheets exposed at the same time to the same beam and analyzed after different periods.

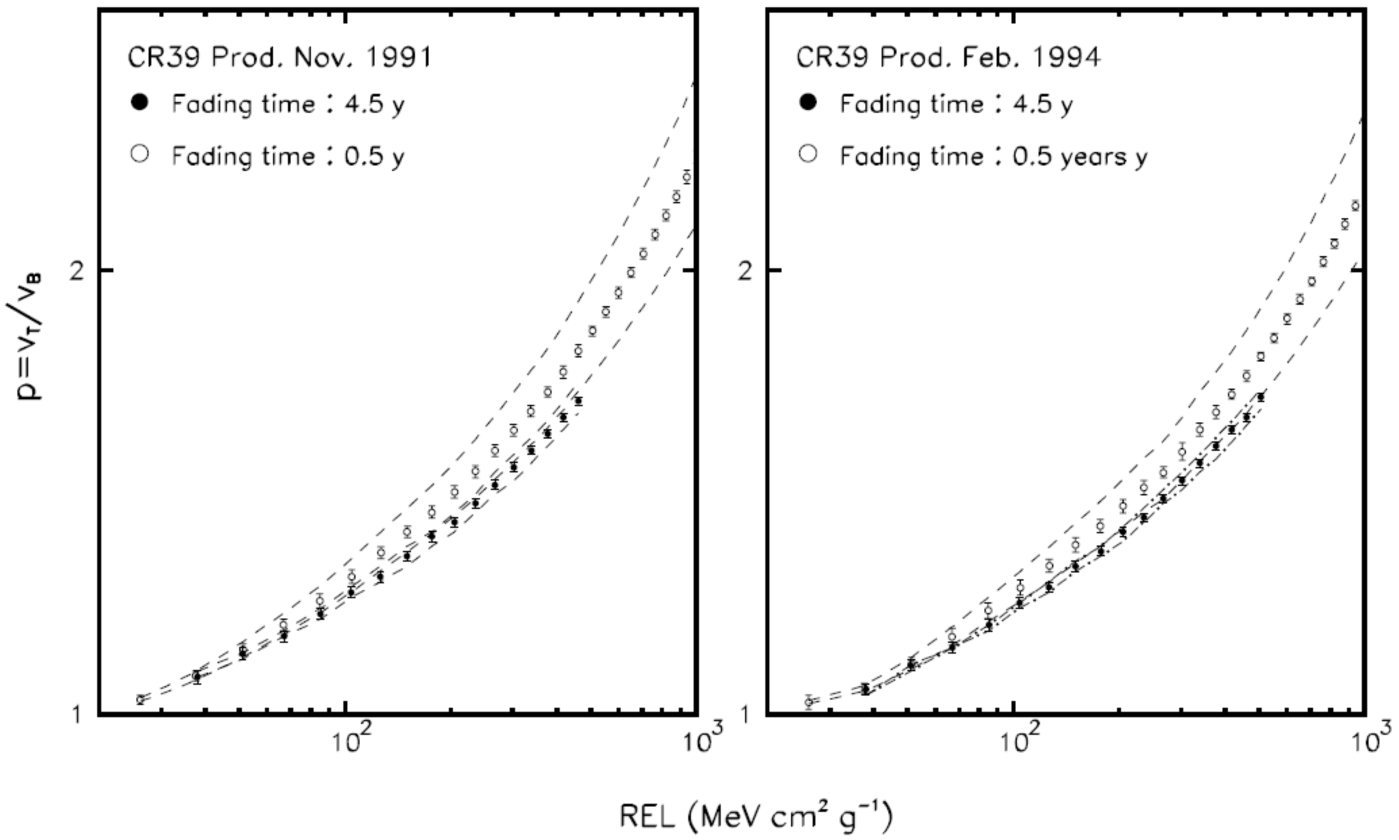

- Several samples belonging to the same production batch were exposed in Dec. 94 to the 158 A GeV lead ion beam and etched after different times (0.5 y and 4.5 y after the exposure).
- The response of the samples etched 4.5 y after exposure is less than 10% lower than that for the samples etched shortly after.
- The difference is within experimental uncertainties on bulk velocity, shown as bands in Figure.

Conclusions

- The MACRO and SLIM experiments were strongly motivated by theoretical arguments
- In MACRO, **redundancy** and **complementarity** were the primary features in designing the experiment: it was deemed crucial to have multiple signatures to claim detection on the passage of a single MM
- The NTD subsystem with the INTERCAST CR39 was one of the three main elements of MACRO and the core of the SLIM experiments, covering a wide range of MM mass, magnetic charge, and velocity.
- The MACRO CR39 covered **>1250 m^2** for more than 8y; The SLIM CR39 covered **>400 m^2** for 4y
- The “CR39 -Bologna group” was made possible not only from the clever leadership (prof. Giorgio Giacomelli and dr. Laura Patrizii) but also for certain favorable and probably once-in-a-lifetime situations:
  - The existence of a close by industry (INTERCAST) very collaborative and open to research;
  - The availability of full-time technicians trained to analyze images (former: bubble-chamber pictures).
- The plastic need a long developing time to demonstrate the possible use as NTD
- The situation for using NTDs is different in underground and mountain-level laboratories
- The etching of massive quantity of plastic need dedicated environmental attention
- The improvement in the machine learning analysis can significantly fasten the scanning time

Notable references

1. R. L. Fleischer, P. B. Price, and R. M. Walker. *Nuclear Tracks in Solids: Principles and Applications* University of California Press, Berkeley, 1975
2. G. Giacomelli. *Magnetic Monopoles*. La Rivista del Nuovo Cimento 7:12 (1984)
3. L. Patrizii, M. Spurio, *Status of Searches for MM*. Annu. Rev. Nucl. Part. Sci. 2015. 65:279–302
4. MACRO Coll., *Final results of MM searches with the MACRO experiment.* Eur. Phys. J. C 25, 511 (2002)
5. S. Cecchini et al., *Calibration with relativistic and low-velocity ions of a CR39 nuclear track detector*. Nuovo Cimento A 109, 1119 (1996)
6. Ziegler J. F., Biersack J. P., Littmark U., *The Stopping and Range of Ions in Solids* (Pergamon Press) 1985.
7. Y. D. He. *Can track-etch detector CR-39 record low-velocity GUT magnetic monopoles?* PRD57(1988) 3192
8. S. Cecchini et al., *New calibrations and time stability of the response of the INTERCAST CR39.* Rad. Meas., 34(2001)54
9. S. Balestra et al. (SLIM). *Magnetic monopole search at high altitude with the SLIM experiment.* EPJ. C 55, 57–63 (2008)
10. S. Balestra et a. *The treatment and rejection of two "strange" candidate events in the SLIM experiment.* arXiv:0802.2056
11. S. Manzoor, PhD Thesis. University of Bologna
12. J. Derkaoui et al., *Energy losses of magnetic monopoles and of dyons in the earth*. Astroparticle Physics 9 (1998) 173
13. J. Derkaoui et a., *Energy losses of magnetic monopoles and dyons in scintillators, streamer tubes and nuclear track detectors*. Astroparticle Physics 10 (1999) 339

Spares

Accuracy of the TRIM Code: measurement of the range

TABLE II. – *Ranges of 200 keV protons, 100 keV deuterons, 300 keV* Be^{2+} *and 400 keV* Si^{2+} *ions as predicted by the TRIM code* (R_{TRIM}) *and as experimentally measured* (R_{exp}). *The samples were etched beyond the ion end-of-range.*

Ion	E (keV)	t_{etch} (h)	R_{exp} (μm)	R_{TRIM} (μm)
H	200	14	2.10 ± 0.11	2.2
D	100	9	1.24 ± 0.10	1.38
$^{9}Be^{2+}$	300	5	1.30 ± 0.13	1.27
$^{28}Si^{2+}$	400	3	0.82 ± 0.09	0.84

Nuclear track detectors for magnetic monopole searches in large area experiments

Maurizio Spurio (maurizio.spurio@unibo.it)

Università di Bologna and INFN